ELSEVIER

International Journal of Solids and Structures 41 (2004) 3383–3393

INTERNATIONAL JOURNAL OF SOLIDS and STRUCTURES

www.elsevier.com/locate/ijsolstr

Caustic study on stress singularities in laminated composites under concentrated loads

X.F. Yao [a,*], W. Xu [a], M.Q. Xu [a], G.C. Jin [a], H.Y. Yeh [b]

[a] *Department of Engineering Mechanics, Tsinghua University, Qinghua Yuan, Hai Dian District, Beijing, 100084, China*
[b] *Department of Mechanical and Aerospace Engineering, California State University, Long Beach, CA 90840-8305, USA*

Received 28 January 2004; received in revised form 28 January 2004
Available online 12 March 2004

Abstract

The local stress singularities of laminated composite materials under concentrated loads are studied by the optical method of caustics. The parametric equation of the caustics and its initial curve surrounding the stress concentration zone are derived from the theoretical closed-form elastic solutions and the principle of reflective caustics. Theoretical formulae of determining the relation between the local concentrated load and the geometric characteristic size of caustic curve are obtained. Theoretical caustics and initial curves for laminate orthotropic composites are simulated and analysed. To compare with the numerical results, a dynamic caustic experiment by means of multi-spark high-speed camera is performed to investigate the dynamic evolution of local stress singularities in laminated carbon fibre/epoxy composites subjected to impact-concentrated loading.

Keywords: Composites; Optical caustics; Local stress singularities; Concentrated load

1. Introduction

The widely application of fiber-reinforced composites in the field of the aerospace and automotive industries is due to the fact that these materials have a very high stiffness to weight ration, high strength to weight ratio, and impact resistance. In practise, the concentrated load is often used during the service of composite structures, which will cause the stress concentration and induce the local failure near the concentrated load zone. Therefore, the study of stress singularity of composites subjected to concentrated load is an important subject in evaluating strength and predicting service life for composite structures.

However, due to the anisotropy and nonhomogeneous of composite materials in meso/micro-scale level, the stress singularity of composite is different from that of traditional isotropic material. Trace to its source, the stress distribution in a half-plane orthotropic plate under a concentrated load was firstly derived by Green (1945). This solution was first used to the problem of an isolated force acting on an internal point of

* Corresponding author. Tel.: +86-10-62771546; fax: +86-10-62781824.
E-mail address: yxf@mail.tsinghua.edu.cn (X.F. Yao).

0020-7683/$ - see front matter © 2004 Elsevier Ltd. All rights reserved.
doi:10.1016/j.ijsolstr.2004.02.007

an infinite anisotropy plate and determine the stress distribution of some anisotropy materials such as oak and spruce. In these stress expressions, the stress singularity of order $1/r$ appeared, which has a direct relation with anisotropic material constants and applied load. In view of the difficulty of theoretical analysis for composite stress singularity, experimental study has become an important tool. Among most experimental techniques, the optical method of caustics has been proved to be very effective for the study of stress singularities, as well as any other type of stress discontinuities or concentrations due to either the change of the applied load or the specimen geometry (Kalthoff, 1987; Rosakis, 1980; Aawakawa et al., 2000; Yao et al., 2002, 2003). The advantages of this experimental method lie in the simple optical patterns, which can establish the relation between the stress field parameters and the characteristic size of caustic curve. So far this method has been successfully used to study the stress concentrated problems for isotropic material, such as the stress singularity at crack tip, stress concentration around small holes, and stress concentration of half-plane subjected to the concentrated-edge load. But for the anisotropy materials, the caustic method is only used to study the stress singularity of crack tip due to composites' opaque character. Theocaris (1976) studied the transversing anisotropy plate with stationary crack under in-plane loading and analysed the stress concentration in anisotropy plates by the method of caustics. Semenski (1997), Semenski and Jecic (1998) derived the equation of caustic and initial curve of the crack tip using the crack elastic solution of rectilinear anisotropy bodies, which was first given by Sih et al. (1965), and compared the simulated caustic image with the experimental obtained caustic curve. Theocaris and Georgiadis (1984) evaluated mode III stress intensity factor (SIF) of stationary cracks in orthotropic plates by the caustics. Based on the author's knowledge, so far there is no literature discussion about the application of caustic method to the study of dynamic stress singularities of composite materials in half-plane subjected to concentrated-edge load.

In this paper, the reflective optical caustic method is used to study the stress singularity in laminated composites under the concentrated-edge load. The parametric equations of the singular caustics and its initial curve surrounding the stress concentration zone are derived. The relations between the applied concentrated load and the maximum transverse diameter of caustic curve are established. Some typical caustics and their initial curves for different composites are modelled. Dynamic optical caustic experimental results of epoxy/carbon fiber composite under the concentrated impact loading are presented. The initial damage generation and the subsequent evolution of dynamic failure around the concentrated-loading zone are visualized by the optical shadow spots.

2. The stress field of an orthotropic half-plane subjected to a concentrated-edge load

In order to obtain the quantitative analysis result from the caustic experiment on composite, an analytic expression of the local stress field due to the concentrated load zone is required. In this section, considering a load P applied perpendicular to the edge of an orthographic half-plane as shown in Fig. 1, Green (1945) has given the stress components for generalized plane stress as

$$\sigma_r = \frac{P\sin\theta}{2\pi(\alpha_1-\alpha_2)s_{22}r}\left\{\frac{\alpha_1^{-\frac{1}{2}}(s_{12}-\alpha_1 s_{22})\{3\alpha_1-1+(\alpha_1-1)\cos 2\theta\}}{\alpha_1+1+(\alpha_1-1)\cos 2\theta} - \frac{\alpha_2^{-\frac{1}{2}}(s_{12}-\alpha_2 s_{22})\{3\alpha_2-1+(\alpha_2-1)\cos 2\theta\}}{\alpha_2+1+(\alpha_2-1)\cos 2\theta}\right\} \tag{1}$$

$$\sigma_\theta = 0 \tag{2}$$

$$\tau_{r\theta} = \frac{P\cos\theta}{2\pi(\alpha_1-\alpha_2)s_{22}r}\left\{\alpha_1^{-\frac{1}{2}}(s_{12}-\alpha_1 s_{22}) - \alpha_2^{-\frac{1}{2}}(s_{12}-\alpha_2 s_{22})\right\} \tag{3}$$

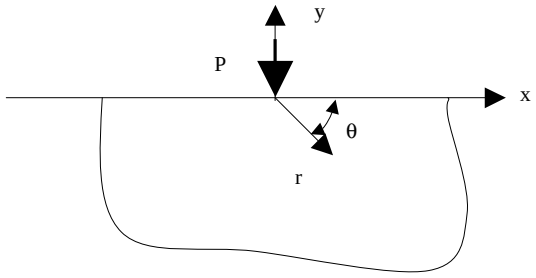

Fig. 1. Compressive-edge loads on half-plane.

where r is the polar radius and θ is the polar angle for the given measured position. α_1, α_2 are given by

$$\alpha_1\alpha_2 = s_{11}/s_{22} \quad \alpha_1 + \alpha_2 = (s_{66} + 2s_{12})/s_{22} \tag{4}$$

with

$$s_{11} = 1/E_1 \quad s_{22} = 1/E_2 \qquad s_{66} = 1/G_{12} \quad s_{12} = -v_{21}/E_1 \tag{5}$$

Here the footnote 1, 2 represents the principle axes of the material in the longitudinal and transverse directions, respectively. E_1 and E_2 are the principal Young's moduli, G_{12} is the corresponding in-plane shear stiffness and v_{12} is the in-plane Poisson's ratio.

According to the constitutive equation for the linear elastic orthotropic composites in the case of the plane stress, the following relation is expressed as

$$\varepsilon_3 = (s_{13}\cos^2\theta + s_{23}\sin^2\theta)\frac{P\sin\theta}{r}(mC - nD) + 2\sin\theta\cos\theta(s_{23} - s_{13})\frac{P\cos\theta}{r}(m - n) \tag{6}$$

where

$$(\alpha_1 - 1)\cos 2\theta = A \quad (\alpha_2 - 1)\cos 2\theta = B$$

$$\frac{3\alpha_1 - 1 + A}{\alpha_1 + 1 + A} = C \quad \frac{3\alpha_2 - 1 + B}{\alpha_2 + 1 + B} = D$$

$$\frac{\alpha_1^{-\frac{1}{2}}(s_{12} - \alpha_1 s_{22})}{2\pi(\alpha_1 - \alpha_2)s_{22}} = m \quad \frac{\alpha_2^{-\frac{1}{2}}(s_{12} - \alpha_2 s_{22})}{2\pi(\alpha_1 - \alpha_2)s_{22}} = n$$

$$s_{23} = \frac{-v_{32}}{E_2} \quad s_{13} = \frac{-v_{31}}{E_1} \tag{7}$$

Here ε_3 is the strain component. v_{31} and v_{32} are the out of plane Poisson's ratio.

Let

$$s_{13}\cos^2\theta\sin\theta + s_{23}\sin^3\theta = U \tag{8}$$

$$(s_{23} - s_{13})\sin\theta\cos^2\theta = V \tag{9}$$

Eq. (6) becomes

$$\varepsilon_3 = \frac{P}{r}[U(mC - nD) + 2V(m - n)] \tag{10}$$

3. Caustic parametric equation of local stress concentration zone in orthotropic material

According to the caustic method, the stress singularity is transformed into an optical singularity, expressed by the caustics, whose shape and dimensions yield sufficient information for evaluation of the stress field at the close vicinity of the singularity. When a light beam (parallel, convergent or divergent) illuminates on the lateral faces of an anisotropic plate subjected to a concentrated load, it will be reflected from the surface of the specimen and received on the reference plane at a distance Z_0 from the specimen (see Fig. 2). The reflected caustic with a dark spot surrounded by a bright curve at its edge is obtained on the reference plane. Here, the correspondence relation between the points $P(X, Y)$ on the reference plane and $p(x, y)$ on the specimen plane is established by

$$X = \lambda x + Z_0 d \frac{\partial \varepsilon_3}{\partial x} \tag{11}$$

$$Y = \lambda y + Z_0 d \frac{\partial \varepsilon_3}{\partial y} \tag{12}$$

where λ is a scale factor (parallel light $\lambda = 1$, convergent light $\lambda < 1$ or divergent light $\lambda > 1$), and d is the effective thickness of specimen.

By substituting Eq. (10) into Eqs. (11) and (12), we can obtain

$$X = \lambda r \cos\theta - Z_0 d P r^{-2}\left[\left(\cos\theta U + \sin\theta \frac{\partial U}{\partial \theta}\right)(mC - nD) + 2(m-n)\left(V\cos\theta + \sin\theta \frac{\partial V}{\partial \theta}\right) + U\sin\theta\left(m\frac{\partial C}{\partial \theta} - n\frac{\partial D}{\partial \theta}\right)\right] \tag{13}$$

$$Y = \lambda r \sin\theta - Z_0 d P r^{-2}\left[\left(\sin\theta U - \cos\theta \frac{\partial U}{\partial \theta}\right)(mC - nD) + 2(m-n)\left(V\sin\theta - \cos\theta \frac{\partial V}{\partial \theta}\right) - U\cos\theta\left(m\frac{\partial C}{\partial \theta} - n\frac{\partial D}{\partial \theta}\right)\right] \tag{14}$$

From the formation principle of caustics, it can be concluded that the caustics is a strongly illuminated singular curve. The necessary condition of existence of such a singularity is that the Jacobian functional determinant J equals zero, i.e.

$$J = \frac{\partial(X, Y)}{\partial(r, \theta)} = \begin{vmatrix} \frac{\partial X}{\partial r} & \frac{\partial X}{\partial \theta} \\ \frac{\partial Y}{\partial r} & \frac{\partial Y}{\partial \theta} \end{vmatrix} = 0 \tag{15}$$

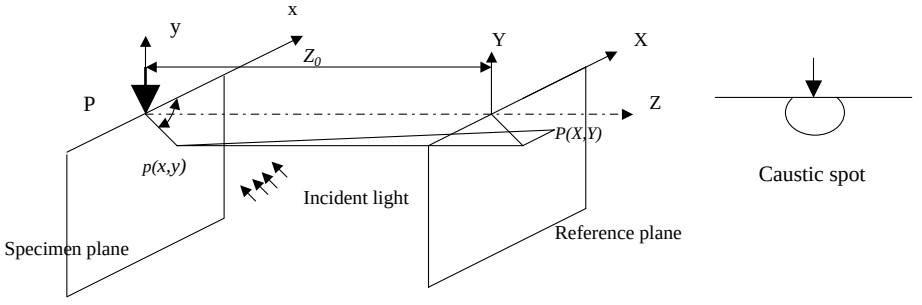

Fig. 2. Geometrical conditions of the shadow optical analysis with reflective.

By introducing Eqs. (13) and (14) into Eq. (15), we have

$$\lambda^2 r + Z_0 dPr^{-2}\lambda E + 2(Z_0 dP)^2 r^{-5} F = 0 \tag{16}$$

where

$$E = \left(U + \frac{\partial^2 U}{\partial\theta^2}\right)(mC - nD) + 2\frac{\partial U}{\partial\theta}\left(m\frac{\partial C}{\partial\theta} - n\frac{\partial D}{\partial\theta}\right) + 2(m-n)\left(V + \frac{\partial^2 V}{\partial\theta^2}\right) + U\left(m\frac{\partial^2 C}{\partial\theta^2} - n\frac{\partial^2 D}{\partial\theta^2}\right)$$

$$F = -2\left[\frac{\partial U}{\partial\theta}(mC - nD) + U\left(m\frac{\partial C}{\partial\theta} - n\frac{\partial D}{\partial\theta}\right) + 2\frac{\partial V}{\partial\theta}(m-n)\right]^2 + [U(mC - nD) + 2V(m-n)]$$
$$\times\left[\left(\frac{\partial^2 U}{\partial\theta^2} - U\right)(mC - nD) + 2\left(\frac{\partial^2 V}{\partial\theta^2} - V\right)(m-n) + 2\frac{\partial U}{\partial\theta}\left(m\frac{\partial C}{\partial\theta} - n\frac{\partial D}{\partial\theta}\right) + U\left(m\frac{\partial^2 C}{\partial\theta^2} - n\frac{\partial^2 D}{\partial\theta^2}\right)\right]$$

The solution of Eq. (16) leads to the function $r_0 = r(v_{31}, E_1, \theta, \lambda, Z_0, P, d, E_2, \ldots)$, which represents the initial curve positioned on the specimen surface. The equation of the initial curve at the crack tip can be written as

$$r = \sqrt[3]{\frac{Z_0 dP}{\lambda}N} \tag{17}$$

where

$$N = \frac{4F}{-E - \sqrt{E^2 - 8F}} \tag{18}$$

By introducing Eq. (17) into Eqs. (13) and (14), the parametric equations of the caustics can be expressed as

$$X = \lambda^{\frac{2}{3}}(Z_0 dP)^{\frac{1}{3}}\left\{N^{\frac{1}{3}}\cos\theta - N^{-\frac{2}{3}}\left[\left(\cos\theta U + \sin\theta\frac{\partial U}{\partial\theta}\right)(mC - nD) + 2(m-n)\left(V\cos\theta + \sin\theta\frac{\partial V}{\partial\theta}\right)\right.\right.$$
$$\left.\left. + U\sin\theta\left(m\frac{\partial C}{\partial\theta} - n\frac{\partial D}{\partial\theta}\right)\right]\right\} \tag{19}$$

$$Y = \lambda^{\frac{2}{3}}(Z_0 dP)^{\frac{1}{3}}\left\{N^{\frac{1}{3}}\sin\theta - N^{-\frac{2}{3}}\left[\left(\sin\theta U - \cos\theta\frac{\partial U}{\partial\theta}\right)(mC - nD) + 2(m-n)\left(V\sin\theta - \cos\theta\frac{\partial V}{\partial\theta}\right)\right.\right.$$
$$\left.\left. - U\cos\theta\left(m\frac{\partial C}{\partial\theta} - n\frac{\partial D}{\partial\theta}\right)\right]\right\} \tag{20}$$

Finally, the polar radius ρ and the polar angle φ of caustics on the screen plane can be defined by the following relation

$$\rho = \sqrt{X^2(r,\theta) + Y^2(r,\theta)} \tag{21}$$

$$\tan\varphi = \frac{Y(r,\theta)}{X(r,\theta)} \tag{22}$$

4. Simulation of initial and caustic curve on local stress concentrate field in orthotropic composites

From Eqs. (19) and (20), it can be concluded that the situation of stress singularity of orthotropic composites subjected to the compressive-edged load becomes more complicated than that in the isotropic

materials due to its anisotropy term in these equations. The shape of caustics and its initial curve depends heavily on the mechanical properties of orthotropic materials, while its size depends on the arrangement of the experimental set-up and load intensity applied to the specimen.

For the numerical simulation of the caustic and initial curve, the elastic constants of two kinds of composites used for numerical examples are listed in Table 1, which are obtained by the electronic strain gauge technology in our laboratory. These materials are generally orthotropic composites.

The theoretically generated initial curves and caustic curves of two different orthotropic materials are shown in Fig. 3. The comprehensive effect of the material properties on the stress singularity around local

Table 1
Elastic properties of orthotropic composites used for numerical examples

Material	Type	E_{11} (GPa)	E_{22} (GPa)	G_{12} (GPa)	v_{12}	v_{31}	v_{32}
1	A	31.79	38.12	28.12	0.45	0.32	0.34
2	B	34.86	31.42	27.56	0.38	0.28	0.3

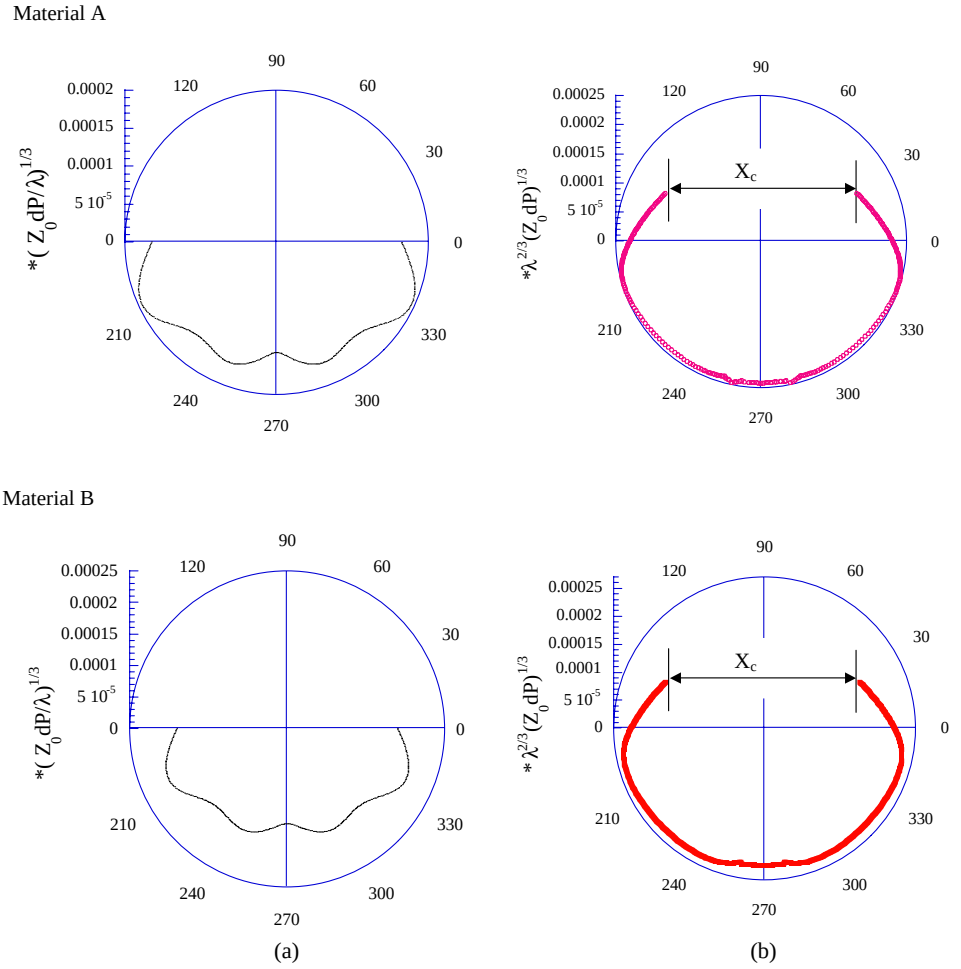

Fig. 3. Theoretical initial curve and caustic curve of two different laminates materials. (a) Initial curve; (b) Caustics.

zone is reflected by the shape, the size of the initial curve and the caustic curve. Once the material properties are known, the caustic shape of the stress concentrated zone is also defined, the size changes proportionally to the amplitude of applied load.

From Fig. 3 it can be observed that initial curve and caustics of local stress concentrated zone for composites show a distinct difference in comparison with the case of complete isotropic materials (Kalthoff, 1987). The former indicates that the initial curve and the singular caustic curve for the case of concentrated loads at the straight boundary of a half-plane are not smooth, while the latter shows a smooth curve.

For different general orthotropic composite materials, the shape of caustics is of the different forms; also the change of the sizes depends on the material properties of orthotropic composites under the same condition of optical set-up and loading.

5. Relation between the applied compressive load and local stress singularities

From the geometrical pattern of caustics in Fig. 3, the upmost transverse distance of caustics can be used as the characteristic parameters for evaluating the stress singularity quantitively. In order to obtain the upmost transverse distance X_c of the caustics as shown in Fig. 3(b), the two positions of θ_1 and θ_2 in the specimen plane corresponding to the X_c of caustic curve are considered as $-\pi$ and 0. In the meantime, the two positions of φ_1 and φ_2 corresponding to the X_c of caustic curve on the reference plane can also be obtained by Eq. (22) as shown in Table 2. And, the caustics is symmetrical to the initial loading direction.

So X_c can be written in the simplest form

$$X_c = \lambda^{\frac{2}{3}}(Z_0 dP)^{\frac{1}{3}}\delta_c \tag{23}$$

where δ_c is a correction factor given by

$$\delta_c = \delta_{\theta_1} - \delta_{\theta_2} \tag{24}$$

with

$$\delta_{\theta=\theta_1,\theta_2} = \left\{ N^{\frac{1}{3}}\cos\theta - N^{-\frac{2}{3}}\left[\left(\cos\theta U + \sin\theta \frac{\partial U}{\partial \theta} \right)(mC - nD) + 2(m-n)\left(V\cos\theta + \sin\theta \frac{\partial V}{\partial \theta} \right) + U\sin\theta \left(m\frac{\partial C}{\partial \theta} - n\frac{\partial D}{\partial \theta} \right) \right] \right\} \tag{25}$$

The factor δ_c for all kinds of complete isotropic materials in the reflective caustics has been proved to be constant. But the simulated results of caustic analysis for different composites revealed this δ_c has a direct relation with material properties and must be calculated for each material separately (see Table 2). Finally, the relation between the local concentrated load P_c and the upmost transverse distance X_c of the caustics can be expressed as

Table 2
θ_1 and θ_2, φ_1, φ_2, and δ_{max} for two orthotropic composites

Material	Type	θ_1 (°)	θ_2 (°)	φ_1 (°)	φ_2 (°)	δ_c
1	A	180	0	153.6	26.4	3.30×10^{-4}
2	B	180	0	152.4	27.3	3.51×10^{-4}

$$P_c = \frac{1}{z_0 d \lambda^2} \left(\frac{X_c}{\delta_c} \right)^3 \tag{26}$$

Therefore, it is only required to measure the characteristic diameters of the caustics for the given testing material in the experiment, then the local concentrated load can be determined.

6. Experimental results and discussion

In order to verify the theoretical caustics around the local zone stress field for orthotropic composites, dynamic optical caustic experiments of carbon fiber laminated composites are performed subjected to the concentrated-edge loading. The impact model configurations of the laminated specimen are shown in Fig. 4(a). The mechanical properties of the materials are given as Material A and B in Table 1. The dimension of the specimen is 0.12 m × 0.03 m × 0.003 m for Material A and 0.12 m × 0.03 m × 0.004 m for Material B in length × height × width, respectively. The fiber volume fraction of the two specimens is approximately 52% for Material A and 58% for Material B, respectively.

Due to the non-transparent of the composites, the surface of the specimen need be prepared by the following procedure: an optically flat glass plate is coated with thin aluminium of 500 Å thickness. The coated glass is then affixed to the sample using an epoxy adhesive, which glues the coated surface of the optically flat glass to the sample. The epoxy adhesive is a mixture of epoxy resin and hardener. After the epoxy cured, the glass was peeled off, and then a thin reflective coating was transferred to the surface with epoxy resin for the reflective. The total thickness of the epoxy layer and the coating is just a couple of microns. Compared with the sample thickness, this layer is very thin and will not affect the deformation state inside the specimen.

The specimen was mounted in a drop weight tower with a 3 kg free-failing weight and 900 mm height, which is able to provide impacts at low loading rates. The experimental optical equipment of multi-spark high speed camera is shown in Fig. 4(b), which consisted of 4×4 array point light source S, field lens F and half-reflective lens M and 4×4 array cameras L. In this equipment, the output aperture of the spark gap should be as small as possible to produce a point light source for obtaining the caustic spot. The light from each spark is first reflected by the mirror surface of the specimen, and entered into the camera where the specimen off-focused images are obtained. Synchronizations of the impact load with the sparks are achieved by means of a time sequence controlled circuit. In this test, the distance Z_0 between the reference plane R and the specimen plane is 0.65m. On the other hand, the force transducer between the loading dart tip and the steel rod is used to record the dynamic history of applied impact load.

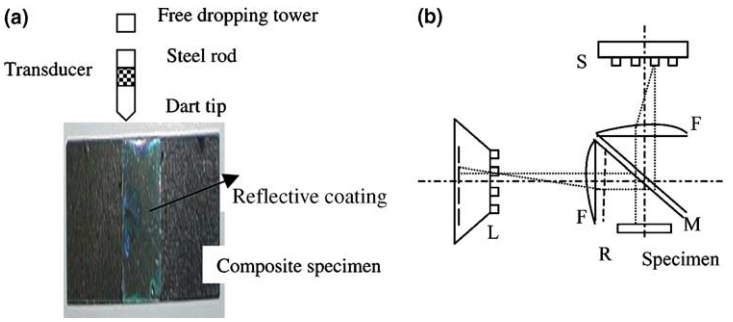

Fig. 4. Dynamic test. (a) Impacted specimen; (b) A modified Cranz-schardin camera.

During the whole testing work, dynamic experiments on two kinds of composites were performed under impact loading. After impact, intensive stress waves emanate from the loading point and propagating toward the specimen. The complex stress field are thus built up surrounding the concentrated loaded zone.

A series of experimental caustics for different loading instants are recorded for two kinds of materials, respectively. Figs. 5 and 6 show the typical dynamic caustic image patterns for Material A and Material B. Their interval frame time is 10 μs. According to the method of caustics, the light rays impinging normally at the specimen and the reflected rays from the front face of the specimen are deviated because of the important constraint of the specimen at the vicinity of the applied load. The deviated light rays, when projected on a reference screen, are concentrated along a singular curve, which is strongly illuminated and forms a caustic. Their geometrical shapes and sizes are different from that of isotropic material, which depends strongly on the mechanical properties of the orthotropic material, and the load intensity. The size of caustics surrounding the concentrated load zone can characterize the intensity of the applied load. Since the specimen was normally loaded on the edge, the caustic is basically symmetrical.

These experimental caustic images are basically resembled as the theoretical modelling caustic patterns as shown in Fig. 3. The main difference between theoretical and experimental result lies in the distortion of caustic curve due to anisotropy effects on the stress distribution at local concentrated zone in practical test of the composite material. On the other hand, the theoretical modelling of caustic curve is based on the ideal analytic solution. From the viewpoint of the composite structure itself, it can be concluded that the distortion of the caustic edge lies in the influence of the distribution direction of fiber, interface of fiber and matrix, and the mismatch of mechanical properties. In order to obtain the related quantitative mechanics parameters, a specific image analysis software written by C++ language was used to extract the caustic edge using approximately half the maximum intensity point in the diffracted caustic which has ambiguity in the location of the caustic edge due to diffraction effects (Math and Kin, 1986). The utmost transverse distance can be measured from the caustic intensity profile across the caustic diameter. According to the image processing technology, the utmost transversely distances X_c of caustic spots for different instants are measured and the corresponding applied load P_c are calculated by Eq. (26), which are displayed as function

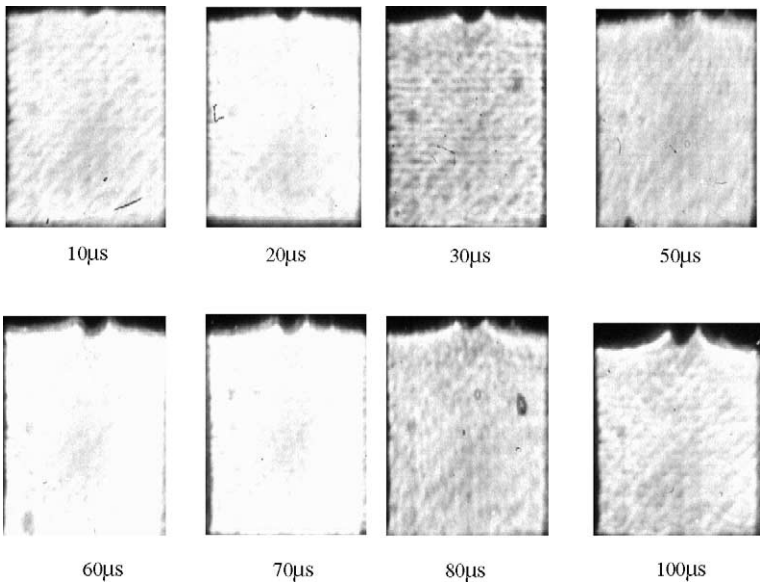

Fig. 5. Caustic patterns in Material A induced by local stress concentration.

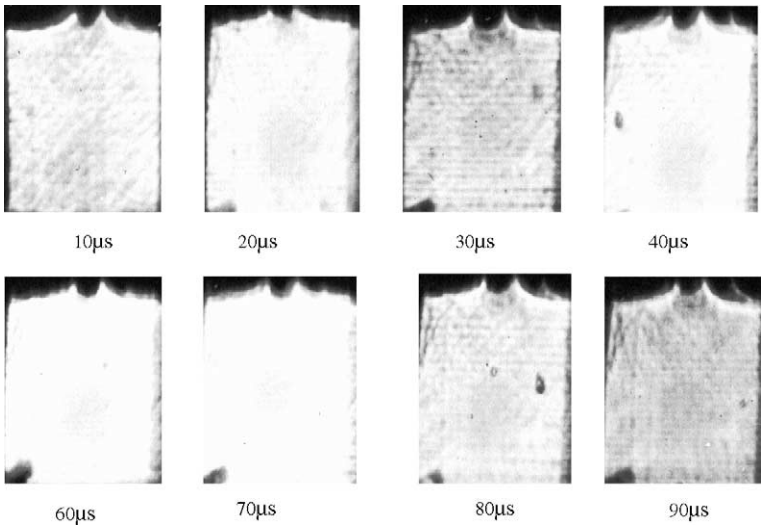

Fig. 6. Caustic patterns in Material B induced by local stress concentration.

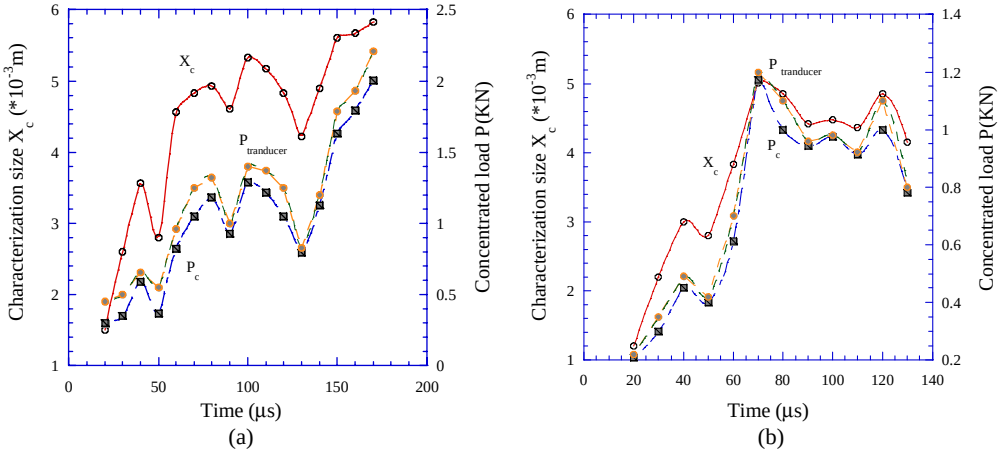

Fig. 7. Dynamic evolution of caustic characterizations and local applied load. (a) Material A; (b) Material B.

of time after impact in Fig. 7. The changes of X_c and P_c reflected the nonlinearity of the local singular stress field evolution during the whole process of dynamic loading. The change of the caustic geometrical size indicates the evolution of the local stress field intensity surrounding the concentrated load zone.

In the meantime, the applied impact load $P_{\text{transducer}}$ obtained by the force transducer were also presented in Fig. 7. It can be seen that there are some differences between the P_c and the $P_{\text{transducer}}$, which attributes to the influence of steel rod dart tip between the transducer and the loading position. During the impact process, some impact energies are absorbed by the steel rod dart. For the composite itself, the interaction of microstructure in composite can result in the successive change of elastic strain energy due to local dynamic stress concentration. However, the change tread of the P_c is almost same as that of the $P_{\text{transducer}}$. Therefore, it can be concluded that the local concentrated load can be obtained by the caustic characteristics size, which is the actual load at the local loading zone in composites.

7. Conclusions

The local stress singularities of orthotropic composites subjected to concentrated-edge load have been studied by the optical reflective caustic technology in this paper. Some valuable conclusions are listed: (1) The caustic patterns of local stress concentrated zone for different composite under edge-concentrated load have direct relation with elastic properties of orthotropic materials and the applied load, which shows the stress singularities near the edge-concentrated load zone. (2) The local concentrated load can be determined by measuring the utmost transversely distance of the caustic spot, which show a good agreement with the result obtained by the force transducer. (3) Dynamic caustic experiments for carbon fiber/epoxy composites under impact loading are performed, and the evolution of dynamic local stress concentration are visualized which shows a good agreement with numerical results. (4) Reflective optical caustic technology is suitable for investigating the local stress concentration in composite materials.

Acknowledgements

This research project was supported by China Nature Science Foundation (No.19902008) and Aeronautical Science Foundation.

References

Aawakawa, K., Mada, T., Takahashi, K., 2000. Correlations among dynamic stress intensity factor, crack velocity and acceleration in brittle fracture. Int. J. Fract. Mech. 105 (2), 311–320.

Green, A.E., 1945. Stress system in aerotropic plates II. Proc. Roy. Soc. Series A. pp. 173–178.

Kalthoff, J.F., 1987. Shadow optical method of caustics, Chapter 9. In: Kobayashi, A.S. (Ed.), Handbook on Experimental Mechanics. Prentice-Hall, Englewood Cliffs, NJ, pp. 430–500.

Math, S.M., Kin, K.S., 1986. Coherent-light shadow spot of a crack under mode I loading: theory and experiment. Exp. Mech. 26 (3), 386–393.

Rosakis, A.J., 1980. Analysis of the optical method of caustics for dynamic crack propagation. Eng. Fract. Mech. 13 (2), 331–347.

Semenski, D., 1997. Method of caustics in fracture mechanics of mechanically anisotropic materials. Eng. Fract. Mech. 58 (1), 1–10.

Semenski, D., Jecic, S., 1998. Experimental caustics analysis in fracture Mechanics of anisotropic materials. Exp. Mech. 39 (3), 177–183.

Sih, G.C., Paris, P.C., Irwin, G.R., 1965. On cracks in rectilinear anisotropic bodies. Int. J. Fract. Mech. 1 (2), 189–211.

Theocaris, P.S., 1976. Stress concentration in anisotropic plates by the method of caustics. J. Strain Anal. 11 (2), 154–160.

Theocaris, P.S., Georgiadis, H.G., 1984. Mode III stress-intensity factors in cracked orthotropic plates-An analogy with propagating cracks in isotropic media. Exp. Mech. 24 (2), 177–183.

Yao, X.F., Jin, G.C., Arakawa, K., Takahashi, K., 2002. Experimental studies on dynamic fracture behavior of thin plates with parallel single edge cracks. Polym. Testing 21 (8), 933–940.

Yao, X.F., Xu, W., Xu, M.Q., Arawaka, K., Mada, T., Takahashi, K., 2003. Experimental study of dynamic fracture behavior of PMMA with overlapping offset-parallel cracks. Polym. Testing 22 (6), 663–670.